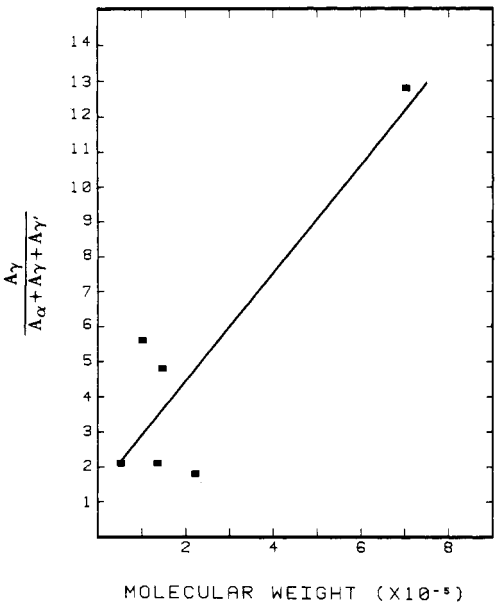

Figure 7. Dependence of the percentage of the γ spherulites in the crystalline regions on the molecular weight for PVF_2 samples crystallized at 433 K for 24 h.

longitudinal propagation is increased. On the other hand, the transformation is impeded by the interlamellar amorphous phase, which acts as a barrier to the transverse propagation. Both the percentage of the γ spherulites in the crystalline regions and the content of the interlamellar amorphous phase increase with the head-to-head defect concentration and the molecular weight. As a result, the degree of the $\alpha \rightarrow \gamma$ transformation appears to be a complicated function of both of these molecular parameters.

Acknowledgment. This work was supported by the Polymers Program of the Office of Naval Research.

Registry No. PVF_2, 24937-79-9.

References and Notes

(1) Lovinger, A. J. *Dev. Crst. Polym.* **1982**, *1*, 195.
(2) Gianotti, G.; Capizzi, A.; Zamboni, V. *Chim. Ind. (Milan)* **1973**, *55*, 501.
(3) Prest, W. M.; Luca, P. J. *J. Appl. Phys.* **1975**, *46*, 4136.
(4) Takahashi, Y.; Tadokoro, H. *Macromolecules* **1980**, *13*, 1316.
(5) Lovinger, A. J. *J. Appl. Phys.* **1981**, *52* (10), 5934.
(6) Lovinger, A. J. *Polymer* **1980**, *21*, 1318.
(7) Chen, L. T.; Frank, C. W. *Ferroelectrics* **1984**, *57*, 51.
(8) Morra, B. S.; Stein, R. S. *J. Polym. Sci., Polym. Phys. Ed.* **1982**, *20*, 2243.
(9) Watkins, K.; Bowker, S. M.; Frank, C. W., submitted to *Macromolecules*.
(10) Takahashi, Y.; Matsubara, Y.; Tadokoro, H. *Macromolecules* **1982**, *15*, 334.
(11) Warner, F. P.; Brown, D. S.; Wetton, R. E. *Polymer* **1981**, *22*, 1349.
(12) Sanchez, I. C.; Eby, R. K. *J. Res. Natl. Bur. Stand., Sect. A* **1973**, *77A*, 353.
(13) Hoffman, J. D.; Weeks, J. J. *J. Res. Natl. Bur. Stand., Sect. A* **1962**, *66A*, 13.

Structural Inhomogeneities in the Range 2.5–2500 Å in Polyacrylamide Gels

Anne-Marie Hecht,† Robert Duplessix,‡ and Erik Geissler*†

Laboratoire de Spectrométrie Physique,§ F-38402 St. Martin d'Hères Cedex, France, and CRM, F-67083 Strasbourg Cedex, France. *Received February 13, 1985*

ABSTRACT: Measurements are presented of the scattering function $S(Q)$ from poly(acrylamide-*co*-bisacrylamide) copolymer gels using light (SLS), small-angle neutron (SANS), and small-angle X-ray (SAXS) scattering. The gels had a fixed acrylamide content (0.08 g/mL) and a bisacrylamide content that varied between 0 and 0.005 g/mL. It is found that all three sets of data can be spliced together to form a single continuous scattering function $S(Q)$, where the scattering wave vector Q lies in the range $4 \times 10^4 \leq Q \leq 1.5 \times 10^7$ cm^{-1}. Contrast variation SANS data show that the spectra can be separated into two parts. The first, a homogeneous solution, gives rise to a quasi-Lorentzian signal with a correlation length ξ that increases with increasing bisacrylamide content. The behavior of $S(Q)$ at high Q values shows that the value of the radius of cross section r_0 of the polymer chains in this phase increases from about 2.5 to 4 Å with increasing bisacrylamide. The total polymer content in this phase is found, however, to be approximately constant. In addition to this homogeneous spectrum, there is also excess forward scattering arising from an inhomogeneous component in the gel, which is characterized by concentration fluctuations of large amplitude. Because of the continuity of $S(Q)$ with the light scattering curves, $S(Q)$ can be calibrated, and one can hence obtain the contribution to the invariant $M_2^{tot} = \int_0^\infty S(Q)Q^2\,dQ$, which is caused by the heterogeneities. Furthermore, in the SANS region of the spectra, the curves follow a fractal behavior, the dimensionality of which is variable at will—by suitable choice of the bisacrylamide content—between 0 and 3.

Introduction

In contrast to polymer solutions, most gels are inhomogeneous structures. The degree of inhomogeneity depends upon the way in which the gel has been formed, and the ultimate strength of these materials is sensitively dependent on such defects. In certain cases, the mechanical properties can be notably enhanced by the artificial introduction of extraneous inhomogeneities, such as silica filler in silicone rubbers. The presence of cross-linking inhomogeneities, on the other hand, promotes brittleness, which for many mechanical applications, is an undesirable characteristic in rubbers.

The effect of cross-linking inhomogeneities on such properties as the permeability of polyacrylamide gels has

† Laboratoire de Spectrométrie Physique.
‡ CRM.
§ CNRS associate laboratory.

0024-9297/85/2218-2167$01.50/0

been the subject of detailed and interesting investigations by Silberberg and co-workers;[1] nonetheless, even when the most restrictive assumption is made, namely that the inhomogeneous gels consist of only two phases, the number of unknown parameters still invariably contrives to exceed that of the independent constituent equations. In this sense, the conclusions drawn from earlier investigations[1-4] must be regarded as model-dependent. In view of the current interest in gel formation, it would appear to be timely to investigate the structures of these gels, as well as of others, using scattering techniques in which the wave-vector range is matched to the expected length scale of the inhomogeneities.

In this paper, we report coordinated observations on a set of polyacrylamide gels using small-angle neutron (SANS), small-angle X-ray (SAXS), and static light scattering (SLS) techniques. As explained below, these different results can be combined to give an overall picture of the deviations from homogeneity in this system.

The information supplied by SANS is of two types. First, the static scattering function of the gel, $S(Q)$, may be explored in a range of transfer wave vectors Q beyond that accessible to SLS techniques and so provides a means of extrapolating these curves. Second, it is a straightforward matter to perform contrast variation experiments, whereby different features in a heterogeneous structure may be suppressed by appropriate matching of the scattering lengths, that is, by varying the proton/deuteron ratio in the surrounding solvent.[5]

When SLS, SANS, and SAXS spectra are fit together on equivalent samples, a composite picture of $S(Q)$ can be obtained for a Q range between about 4×10^4 and 1.5×10^7 cm^{-1}. This is the range in which the structural features appear in polyacrylamide gels that are concomitant with the observed turbidity.

The neutron scattering experiments were performed on the D 11 instrument at the Institut Laue Langevin, Grenoble, while the SAXS measurements were carried out at the LURE synchrotron in Orsay.

Experimental Section

For all the gels described here the materials used were Merck synthesis-grade acrylamide and Merck synthesis-grade *N,N'*-methylenebisacrylamide. These came from the same lot as was used in previously reported experiments on polyacrylamide.[6,7] The appearance of turbidity in these gels, which is the subject of this investigation, is a function of the cross-linking density alone and not of the purity of the materials: such turbidity is also observed with acrylamide from a wide variety of sources.

Immediately after mixing, the precursor fluid was filtered through a 0.22-μm Millipore filter in order to remove any dust particles present and thereupon transferred to the sample cell, where polymerization took place in 10–15 min. The gelation was performed at room temperature (ca. 20 °C) with 0.70 mg/mL of ammonium persulfate and 0.28 μL/mL TEMED. The acrylamide content (A) of the gels was 0.08 g/mL, while the bisacrylamide content (B) varied between 0.005 g/mL for the sample denoted G5 and 0 g/mL for the sample denoted GO (un-cross-linked solution).

The method of preparation of the samples was such that hydrolysis of the acrylamide can be discounted (low TEMED content, short time between preparation and measurements (less than 3 days) and gel pH $\simeq$ 4.5). The small swelling ratios observed[4] and the fact that their characteristic turbidity appears immediately upon gelation both indicate that the precipitation effects described here are unconnected with aging.

The SLS measurements, for samples G0–G3, were made with a Fica apparatus working at 571 nm. Samples G4 and G5, being too turbid for measurements in an apparatus with a long optical path, were made in the form of cylinders of 4-mm diameter, and their scattering patterns were recorded with a He–Ne laser light source. A second sample of G3 of this diameter served as a reference between the two sets of observations.

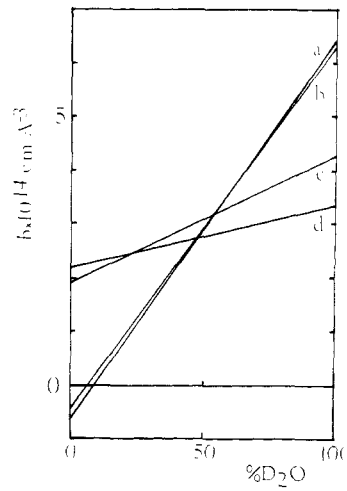

Figure 1. Variation of the neutron coherent scattering length b as a function of deuteron content in the solvent: (a) pure water; (b) solution of 0.08 g/cm^3 water; (c) pure acrylamide; (d) pure bisacrylamide.

The SANS measurements were made on gels 1-mm thick contained in cells with quartz windows, using D_2O as solvent. For the contrast variation observations, the samples were defined by A = 0.08 g/mL and B = 0.003 g/mL and were prepared in water containing respectively 0, 25, 50, 75, and 100% D_2O. The background samples consisted of solutions of unpolymerized acrylamide either in pure D_2O or in the appropriate H_2O/D_2O mixture. Corrections were made separately both for the incoherent background due to the protons in the gel and for residual coherent scattering arising from the quartz windows. Typical counting times were in the range 1–2 h. The incident wavelength was 6.3 Å, and the sample–detector distance was 10.6 m.

For the SAXS measurements, the samples were polymerized in a similar fashion inside cells with thin (ca.5–10 μm) mica windows, separated by a 1.0-mm spacer. The background samples were water. With the D 11 instrument at the DCI synchrotron facility at LURE, Orsay, the counting times were typically 1000 s. The incident wavelength was 1.6 Å, and the sample–detector distance was 1 m.

Results

Contrast Variation Measurements. We consider a set of particles of coherent scattering length b and scattering density $\rho = (1/v)\int b\, dv$ immersed in a medium of mean scattering density $\bar{\rho} = (1/v)\int \bar{b}\, dv$, where v is the volume of the particle. The zero-angle scattering intensity is then proportional to[5]

$$S(0) \propto (\rho - \bar{\rho})^2 \qquad (1)$$

$\bar{b}$ is a linear function of the deuteron content of the solvent (Figure 1). Thus, when $(S(0))^{1/2}$ is plotted as a function of D_2O content, a homogeneous solution of particles should display a straight line, intersecting the horizontal axis at a value of D/H characteristic of the solute/solvent pair. From Figure 1 it can be seen that the deuteron concentration at which the signal from acrylamide (assuming two exchangeable protons) is expected to vanish is 54% on the basis of our measured value for the pure polymer density, namely 1.36 g cm^{-3}.

Figure 2 shows the shape of a typical spectrum from a polyacrylamide gel (G3 in fully deuterated water), plotted as $1/S(Q)$ vs. Q^2. The asymptotic region at large Q yields a straight line, corresponding to the Lorentzian form

$$I_L(Q) = I_L(0)/(1 + Q^2\xi^2) \qquad (2)$$

where ξ is the correlation length of the polymer density fluctuations in the solution.[8]

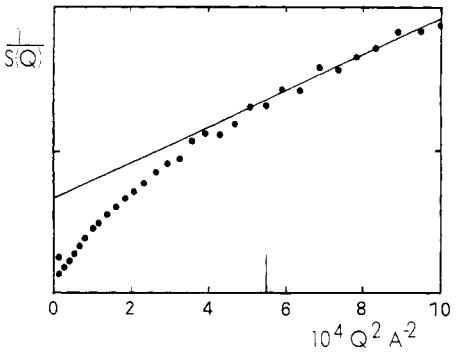

Figure 2. Plot of $1/S(Q)$ against Q^2 of the neutron scattering spectrum from sample G3 with fully deuterated added solvent (i.e., taking account of the exchangeable protons in the acrylamide, 97.8% deuteration of the resultant solvent). The straight line, which is the least-squares fit to the data in the upper wave-vector range ($2.4 \times 10^6 \leq Q \leq 3.2 \times 10^6$ cm^{-1}), indicates a correlation length $\xi = 41$ Å for this sample. Lower bound for fit denoted by bar.

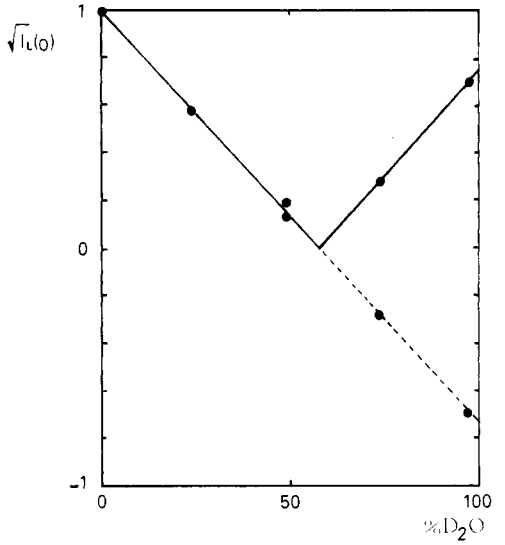

Figure 3. Dependence of the square root of the intensity of the Lorentzian signal $I_L(0)$ as a function of deuteron content of the solvent. The figure is normalized to the intensity scattered by the gel in pure H_2O. The concentration of D_2O at which this signal vanishes is approximately 57%.

In the small-Q region of Figure 2, $1/S(Q)$ deviates increasingly from the asymptotic Lorentzian of eq 2. The excess intensity $I_E(Q)$ is estimated by subtracting from $S(Q)$ the least-squares fit of eq 2 to the high-Q region of the spectrum.

In Figure 3 is shown $(I_L(0)^{1/2}$, expressed relative to the signal from the gel in pure H_2O and plotted as a function of deuterium content in the sample. Within the experimental error, the points lie on a straight line. The compensation concentration at which the signal vanishes is 0.57, compared to the theoretically expected 0.54. This difference is not considered significant, since the theoretical value would coincide with the experimental result if the density of the pure polymer were 1.42 g cm^{-3} instead of 1.36 g cm^{-3}. It should be remembered that the measurement of the density of the dry polymer is subject to errors of about 2%; also, the local density of the polymer in solution can easily exceed the dry bulk value. From Figure 3 we can see that the Lorentzian background signal is strong (it is of comparable intensity to the signal from the un-cross-linked solution) and homogeneous. It must therefore correspond to a phase of essentially uniform composition that occupies a significant fraction of the sample. In what follows, we shall assume that the effective density of polyacrylamide is 1.42 g cm^{-3}.

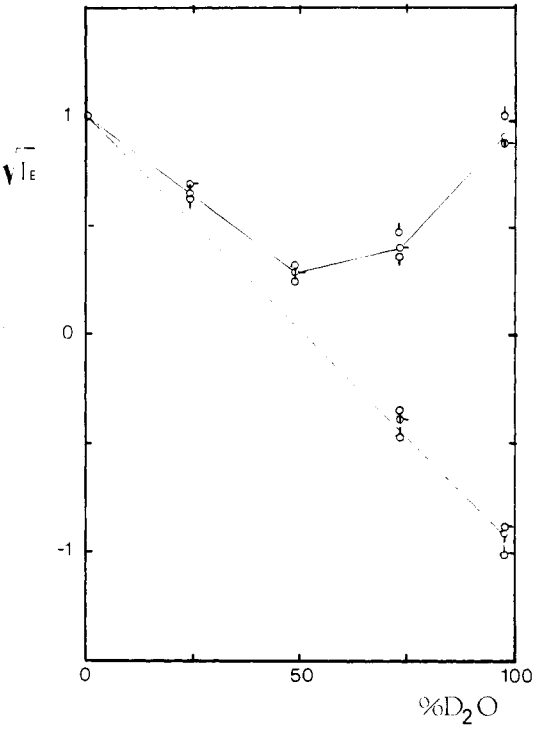

Figure 4. Dependence of the square root of the excess intensity $I_E(Q)$ as a function of deuteron content in the solvent normalized to the corresponding signal from the gels in pure H_2O. The symbols (♁), (○–), and (♀) refer to measurements at $Q = 5.3 \times 10^5$, 9.9×10^5, and 1.3×10^6 cm^{-1}, respectively, each recorded point being the average of the two data on either side of the stated Q value for each spectrum. The continuous straight lines connect average values at $Q = 1.0 \times 10^6$ cm^{-1}, obtained by interpolation on a double-logarithmic representation from the ten lowest Q value data in each spectrum. The discontinuous straight line connects the average points at maximum and minimum D_2O content.

The situation is somewhat modified when one considers the excess forward scattering

$$I_E(Q) = S(Q) - I_L(Q) \tag{3}$$

In principle, when dealing with heterogeneous structures, the quantity of interest is the intensity in the long-wavelength limit $Q \to 0$. In the present case, there is no obvious recipe for extrapolating $I_E(Q)$ to $Q = 0$, since, in the neutron wave-vector range available, $I_E(Q)$ diverges as Q^{-m}, where m is about 2.3. Figure 4 shows the variation of $(I_E(Q))^{1/2}$ vs. deuterium content in the sample for three representative values of Q. No systematic Q dependence is discernable. The experimental points in the range $4.7 \times 10^5 \leq Q \leq 1.3 \times 10^6$ cm^{-1} show a marked deviation from straight-line behavior, betraying the presence of objects of nonuniform scattering density.[2]

Such nonuniformity in the scattering density is not compatible with a model of the gel in which the precipitated phase is composed of either pure pockets of solvent (microsyneresis)[9] or low-concentration solution,[1] or, on the contrary, just of regions of pure polymer,[4] since each of these has a well-defined scattering density and would therefore give rise to a straight line in Figure 4. From Figure 1 it can be seen that the expected signal from pockets of water $[\propto(a - b)^2]$ is much smaller than from either pure acrylamide $[(c - b)^2]$ or pure bisacrylamide $[(d - b)^2]$. By joining the extremal points on Figure 4, an estimate can be made of the isopycnic point of the principal contribution to the excess neutron scattering: the crossover occurs at about 50% deuteron content. If

Table I
Experimental Parameters for Poly(acrylamide-*co*-bisacrylamide) Copolymer Gels Containing 0.08 g/mL Acrylamide

sample	bisacrylamide content, mg/mL	$I_L(0)$, arb units	ξ, Å	$\tilde{M}_2 \times 10^4$ [a]	ρ,[b] e/Å^3	r_0, Å	w_1	ϕ
G0	0	1.0	22		0.458	2.43	0.080	1.000
G1	1.0	1.4	26	0.25	0.475	2.57	0.076	0.997
G2	2.0	1.8	30	1.1	0.490	2.87	0.073	0.985
G3	3.0	3.2	40	5.3	0.532	2.65	0.068	0.928
G4	4.0	5.5	53	6.0	0.583	3.38	0.065	0.918
G5	5.0	8.7	67	18.5	0.636	4.13	0.063	0.75

[a] $\tilde{M}_2$, as defined in eq 19 is a dimensionless quantity. [b] ρ, the electron density of the acrylamide, is calculated from eq 12 and 13, assuming that $\rho_{H_2O} = 0.334$ e/Å^3.

pockets of water were the main source of scattering, the isopycnic point would be at 56% D_2O (assuming that the contrast is between water and a uniform 8% solution of polymer whose dry density is 1.42 g cm^{-3}).

The behavior of the excess forward scattering can be reasonably modeled by assuming the existence of large regions of pure poly(bisacrylamide)[10] (compensation concentration 47%) together with pockets of water; the fit is notably improved if, in addition, the protons of the bisacrylamide are not exchangeable and pure polyacrylamide is included in these regions. The experimental data does not, however, allow a meaningful estimate to be made of the relative proportions of these components. The Q dependence of $I_E(\propto Q^{-2.3})$ excludes the existence of sharp boundaries to these regions, which must therefore be highly folded (fuzzy).

Light, Neutron, and X-ray Scattering Measurements. The samples for these experiments consisted of gels made with 0.08 g/mL acrylamide and varying bisacrylamide content, denoted G0–G5, prepared under identical conditions but in different sample holders. The X-ray and light scattering samples were made with light water, while those for neutron scattering contained pure D_2O.

Our use of the 10-m detector position in the measurements at the ILL means that there is a gap in the observations between the light and the neutron scattering measurements in the region $2.8 \times 10^5 < Q < 4.7 \times 10^5$ cm^{-1}. There is, however, generous overlap with the SAXS range at the high-Q end of the SANS spectra.

Two of the samples, G0 and G2, gave neutron spectra with abnormally low intensities that were inconsistent not only with the spectra from the other samples but also with the relative intensities of the X-ray and the light spectra. We assume that these two deviant spectra suffer either from faulty background subtraction or from errors of preparation. They have been excluded from Figure 5.

Figure 5 shows the combined X-ray, neutron, and light scattering functions for each of the six samples examined. The continuity between each set of data was achieved by sliding the light/neutron and the neutron/X-ray curves vertically with respect to each other in order to obtain a plausible set of smoothly varying curves. Since the vertical scale is logarithmic, this procedure reduces the three types of observation to the same scale factor. The light scattering curve for the sample G0, which was added to Figure 5 after this procedure, coincides satisfactorily with the calculated intensity at $Q = 0$ for the Lorentzian curve corresponding to the same sample from SAXS. The fact that the different scattering curves appear to behave smoothly over more than $2^1/_2$ orders of magnitude of transfer wave vector indicates that it is the same type of density fluctuations that cause the scattering in SLS, SANS, and SAXS. The change in the nature and wavelength of the incident radiation merely alters the total amplitude of the scattering intensity, i.e., generates a shift

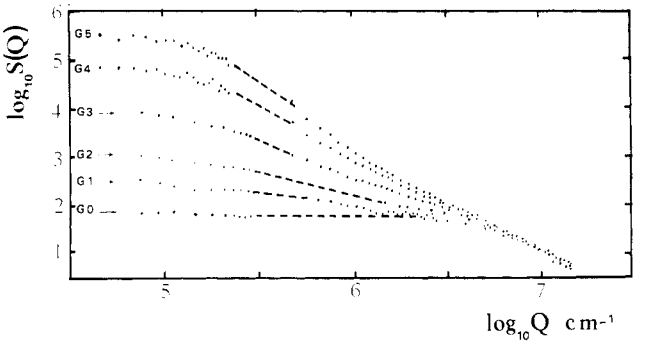

Figure 5. Double-logarithmic representation of the total scattering function $S(Q)$ as a function of Q, obtained from light, neutron, and X-ray scattering, for the series of gels G0 to G5. The scale factor between each type of experimental observation was obtained by sliding each series of curves vertically with respect to each other to obtain a match. The Q vector, which is determined by experimental conditions, cannot be adjusted. The discontinuous straight lines are interpolations. Note that for the X-ray spectra, only a few representative points out of the 256 available for each spectrum have been plotted.

factor, which is subsumed in the matching procedure described above.

The scattering curves of Figure 5 are expressed in arbitrary units. Various ways are available for calibrating this figure, either by using a standard sample in any of the SLS, SANS, and SAXS measurements, or alternatively by measuring the optical turbidity τ of one or more of the samples and comparing the result with the integral[11]

$$\tau = \int_0^\pi S(\theta)(\sin\theta)(1 + \cos^2\theta)\pi \, d\theta \qquad (4)$$

where $S(\theta)$ is given by Figure 5. This second method was the one adopted here.

In Figure 5, it is noteworthy that the slope of the curves at the highest Q values is approximately −2 for all the spectra; i.e., the Porod region of final characteristic slope −4 is not attained in these spectra. This is not a major obstacle for the analysis we present here, since we are principally interested in the differences between spectra.

We start by fitting the data located approximately in the range $3 \times 10^6 \lesssim Q \lesssim 10^7$ cm^{-1} to Lorentzians of the form of eq 2. The resulting values of the correlation length ξ are listed in Table I together with the corresponding values of $I_L(0)$. It can be seen that ξ increases as the bisacrylamide content B increases. This has been reported previously and attributed to a decrease in the concentration of the phase that gives rise to this signal.[4,7] The present results contain new information that allows this conclusion to be examined more critically. Although it is certain that the spacing between polymer strands increases with increasing B, it is also clear from these results that the material in this phase is undergoing structural reorganization. We denote the polymer weight fraction in this phase as w_1. If the structure of the polymer chains com-

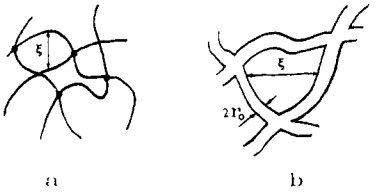

a b

Figure 6. Schematic diagram of proposed structure in the majority (homogeneous) phase of polyacrylamide gels. In gels of low bisacrylamide content (a) the correlation length ξ is small, as is the radius of the chain section, r_0. As the bisacrylamide content increases (b), the chains become both thicker and denser and the separation ξ between chains increases.

posing it remains unchanged on varying B, then the intensity $I_L(0)$ is proportional to the osmotic susceptibility[8]

$$I_L(0) \propto (\rho - \rho_{H_2O})^2/(\partial\mu/\partial w) \propto (\rho - \rho_{H_2O})^2 w_1^2 \xi^3 \quad (5)$$

Now scaling theory predicts that for good solvents

$$\xi \propto w_1^{-0.75} \quad (6)$$

so one expects that

$$I_L(0) \propto \xi^{1/3} \quad (7)$$

The data of Table I indicate on the contrary that

$$I_L(0) \propto \xi^m \quad (8)$$

where m is approximately 2; i.e., the intensity scattered by this phase increases faster than it should if it were simply depleted in polymer content. We conclude that the presence of bisacrylamide produces an increase in the scattering density ρ of the polymer chains. Our picture of this homogeneous phase is that the singly stranded structure prevailing in the polymer solution is replaced, at least in part, by denser bundles of fibers bound together by bisacrylamide, with a larger spacing between bundles (cf. Figure 6).

It is therefore not legitimate to use eq 6 (or any other thermodynamic relation) as the sole definition of the total polymer concentration in this phase since this relation assumes that the polymer structure is invariant as the concentration varies. In order to complete the picture, we need to known how the radius of the fibers r_0 changes with cross-linking density. This information can be obtained from the high-Q range of the SAXS spectra.

When the polymer chain is composed of elements of finite thickness, the scattering function of eq 2 must be modified. We assume for simplicity that the chain has a Gaussian electron-density profile of radius r_0. The corrected scattering function then takes the form[12]

$$I(Q) = \frac{I_L(0)}{1 + \xi^2 Q^2} \exp(-r_0^2 Q^2/2) \quad (9)$$

Equation 9 neglects two additional corrections to $I_L(Q)$, namely the effect of the chain persistence length[12] and the fact that scaling considerations predict that for a polymer in a good solvent, in the intermediate wave-vector region ($Q\xi \geq 2$), the scattering function varies as[8]

$$S(Q) \propto Q^{-5/3} \quad (10)$$

(In a poor solvent, however, $S(Q)$ varies as Q^{-2} in this range.[13]) Either of these effects causes an increase in the scattering intensity over the simple Lorentzian form in the Q range under consideration. The opposite effect, described in eq 9, is observed experimentally (cf. Figure 7). Table I lists the values of r_0 obtained from this fit to the data in the range $2.5 \times 10^6 \leq Q \leq 1.5 \times 10^7$ cm^{-1}. It should be borne in mind, however, that because of our neglect of

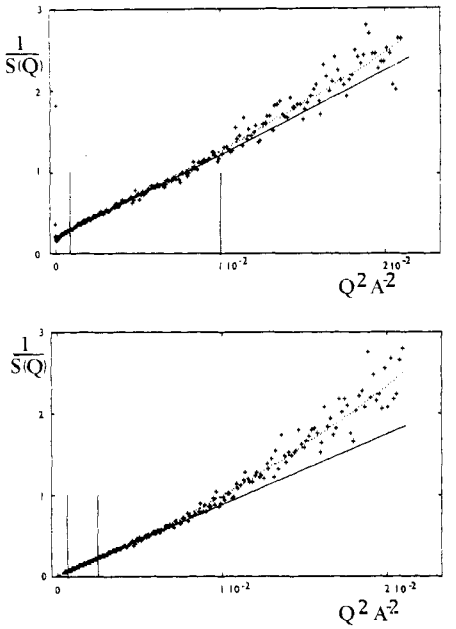

Figure 7. Zimm representation of SAXS spectra from polyacrylamide gels of 0.08 g/cm^3 acrylamide: upper curve, sample G0 (no cross-linking); lower curve, G5 (0.005 g/cm^3 bisacrylamide. The straight lines represent the least-squares fit to the Lorentzian form (eq 2) between the Q limits indicated by the vertical bars. The dotted line represents the least-squares fit to eq 9.

the other two correction factors mentioned above, these values of r_0 are liable to be too small. It is difficult to appreciate the error involved in this estimation of r_0 for two reasons. First, the inclusion of bisacrylamide in the polymerization can be expected to reduce the solubility of the resultant copolymer chains: this introduces an uncertainty into the exponent of eq 10. Second, the residual scatter in the experimental points does not justify the introduction of further unknown parameters. In spite of this rider, there is a clearly discernable trend of increasing r_0 as the cross-linking density increases, in confirmation of the idea expressed in Figure 6.

It is now possible to make a rough estimate of the total polymer concentration w_1 in this phase. We make one further assumption, that the polymer mass density is proportional to the electron density ρ of the polymer chains. Then, defining, for scaling purposes, the apparent concentration of the phase (i.e, the length of polymer chain per unit mass of solution) as

$$\tilde{c} = w_1/\rho r_0^2 \quad (11)$$

one obtains, in place of eq 5 and 6

$$I_L(0) \propto (\rho - \rho_{H_2O})^2 \tilde{c}^2 \xi^3 \quad (12)$$

$$\xi \propto \tilde{c}^{-0.75} \quad (13)$$

In order to reduce the scatter in the values of r_0, we fit the raw data of Table I to a curve of the form

$$r_0^2 \propto \xi^x \quad (14)$$

to obtain

$$x \simeq 0.83 \quad (15)$$

Finally, combining eq 11–15, one obtains

$$w_1 \propto \rho \xi^{-0.5} \quad (16)$$

The values of w_1 calculated from eq 16 are presented in Table I. The resulting variation in w_1 upon cross-linking is rather weak and, given the uncertainties mentioned

above in the estimation of r_0, should be regarded as an upper limit: it is probable that w_1 varies less than indicated in Table I.

It should also be borne in mind that the assumption of good solvent conditions (eq 13) is somewhat doubtful: increasing bisacrylamide content in the gels is known to lower the quality of the solvent. To estimate the effect of this, the same calculations as above may be repeated using the θ condition exponent[13] of −1 in eq 13: the values of w_1 calculated in this way deviate from the unperturbed value by less than 2% (e.g., $w_1 = 0.0786$ for sample G5). We conclude that in the homogeneous phase of these gels, in which the chain structure and the correlation length vary strongly with bisacrylamide content, nonetheless, the polymer weight fraction is hardly different from that in the un-cross-linked solution.

We now turn to the discussion of the rest of the curve $S(Q)$. Clearly, because the Q vector explored does not reach high enough values, it is not possible to calculate its second moment. However, since all the gels have essentially the same composition (the bisacrylamide content, which amounts at most to 6% by weight of the total acrylamide content, can be considered negligible), all the spectra must have the same value of the invariant[14]

$$M_2^{\text{tot}} = \int_0^\infty S(Q)Q^2\,dQ \tag{17}$$

The excess intensity observed in Figure 5 at small Q values over the scattering function for the solution is therefore intensity that has been transferred from $S(Q)$ at values of Q beyond those explored here. The confluence of the $S(Q)$ curves apparent in Figure 5 thus corresponds to the region in which these curves cross over from being above the solution curve to below it. The contribution to M_2^{tot} arising from the low-Q region can be obtained by calculating from Figure 5

$$M_2 = \int_0^{\text{crossover}} \{S(Q) - I(Q)\}Q^2\,dQ \tag{18}$$

where $I(Q)$ may be defined either by eq 2 or 9 with the parameters ξ and r_0 taken from Table I. The resultant values of M_2 are also listed in this table. Note that M_2 as defined in Table I is a normalized value, given by

$$\tilde{M}_2 = \frac{2\tau M_2}{k_0^4 n_0^2 (dn/dw)^2 M_0} \tag{19}$$

where k_0 is the wave vector in vacuo of the incident light at the wavelength at which the turbidity τ is measured, n_0 the refractive index of the gel, dn/dw the refractive index increment,[6] and M_0 the value of the integral appearing on the right-hand side of eq 4 (calculated from Figure 5).

The observed existence of a uniform phase 1 makes it natural to try to interpret the results in terms of a simple two-phase model. However, not only is such a model in disagreement with the contrast variation observations of neutron scattering but it also leads to inconsistent results. We consider instead a variant of the two-phase model, represented schematically in Figure 8. In this model, the principal component, which occupies a volume fraction ϕ of the gel, is the homogeneous phase 1 discussed above; we assume for simplicity that in this phase the polymer weight fraction w_1 is equal to the unperturbed average value $\bar{w}$. The second phase, of volume fraction $1 - \phi$, contains the large-scale spatial concentration fluctuations that give rise to the static scattering observed here.

In line with the contrast variation results, we assume that within the second phase, the polymer weight fraction

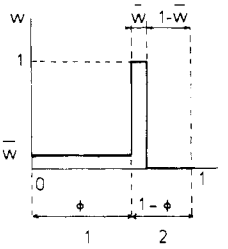

Figure 8. Schematic representation of model concentration distribution in gels: Phase 1, polymer weight fraction $w_1 = \bar{w}$; "phase" 2, concentration fluctuations between $w_2 = 1$ and 0, with $\bar{w}_2 = \bar{w}$.

varies between 0 and 1 but that its average value, $\bar{w}_2$, is the same as that for the whole sample, namely $\bar{w}$. This last assumption is necessary, since the equations are otherwise underdetermined, but not implausible: $w_1 = \bar{w}$ implies that $\bar{w}_2 = \bar{w}$.

It follows that[15]

$$\tilde{M}_2 = \langle \Delta w^2 \rangle = (1 - \phi)\bar{w}(1 - \bar{w}) \tag{20}$$

The resulting values of ϕ are listed in Table I.

It should be stressed that the estimates of both w_1 and ϕ listed in Table I are somewhat model-dependent, but it seems safe to conclude that phase 1 is a majority phase. This conclusion is in agreement with observations of similar gels using dynamic light scattering.[6]

The uniform slope of $S(Q)$ in the lower Q range excludes the possibility of a sharp boundary between phases or components inside the second "phase": on the contrary, a continuous range of characteristics sizes exists, suggestive of fractal behavior.[16] If this description is adopted, the fractal dimensionality D of the heterogeneous "phase" ranges from 0 (polymer solution) to almost 3 (sample G5) in the transfer wave-vector interval $3 \times 10^5 \lesssim Q \lesssim 2 \times 10^6$ cm^{-1}. In particular, the apparent dimensionality of samples G1 and G2 in this range ($D \leq 1$) suggests a dustlike structure for the precipitate,[17] in agreement with the low volume fraction $(1 - \phi)$ calculated for this phase in Table I.

From this investigation of the acrylamide–bisacrylamide copolymer system using light, neutron, and X-ray scattering, the following conclusions can be drawn. The gels contain majority regions of relatively uniform concentration within which the total monomer content is only slightly, if at all, modified. The structure of the polymer chains in this phase is, however, profoundly modified by bisacrylamide, tending to form chains with a higher electronic density and a greater number of monomer units per unit length. In compensation, the average spacing between the chains increases strongly.

In addition to the majority phase, there exists a precipitate of variable composition, which contains regions of high cross-linking density as well as regions of very low polymer content. The spatial structure of this second component displays a fractal behavior in the transfer wave-vector range covered by the small-angle neutron scattering observations. The fractal dimensionality can be varied at will between 0 and 3 by changing the cross-linking density of the gels.

Acknowledgment. It is a pleasure to acknowledge M. Rawiso for several fruitful discussions we have had. We also express our gratitude to S. Bantle, our ILL local contact, to C. Williams and P. Vachette for their invaluable help and advice at LURE, and to M. Milas for the use of the SLS apparatus. We are, of course, totally indebted both to the Institut Laue Langevin, Grenoble and to the

Laboratoire pour l'Utilisation du Rayonnement Electromagnetique at Orsay for the neutron and X-ray facilities.

Registry No. *N,N'*-Methylenebis(acrylamide)·(acrylamide) (copolymer), 25034-58-6; neutron, 12586-31-1.

References and Notes

(1) Weiss, N.; Van Vliet, T.; Silberberg, A. *J. Polym. Sci., Polym. Phys. Ed.* **1979**, *17*, 2229.
(2) Fawcett, J. S.; Morris, C. J. O. R. *Sep. Sci.* **1966**, *1*, 9.
(3) Janas, V. F.; Rodriguez, F.; Cohen, C. *Macromolecules* **1980**, *13*, 977.
(4) Geissler, E.; Hecht, A. M. In "Physical Optics of Dynamical Phenomena and Processes in Macromolecular Systems"; Sedlacek, B., Ed.; de Gruyter: Berlin, 1985; p 157.
(5) Jacrot, B. *Rep. Prog. Phys.* **1976**, *39*, 911.
(6) Hecht, A. M.; Geissler, E. *J. Phys. (Les Ulis, Fr.)* **1978**, *39*, 631.
(7) Geissler, E.; Hecht, A. M.; Duplessix, R. *J. Polym. Sci., Polym. Phys. Ed.* **1982**, *20*, 225.
(8) Daoud, M.; Cotton, J. P.; Farnoux, B.; Jannink, G.; Sarma, G.; Benoit, H.; Duplessix, R.; Picot, C.; de Gennes, P.-G. *Macromolecules* **1975**, *8*, 804.
(9) Dusek, K. In "Polymer Networks"; Chompff, A. J.; Newman, S., Eds.; Plenum Press: New York, 1971; pp 245-260.
(10) Gupta, M. K.; Bansil, R. *J. Polym. Sci., Polym. Lett. Ed.* **1983**, *21*, 969.
(11) Kerker, M. "The Scattering of Light and other Electromagnetic Interactions"; Academic Press: New York, 1969.
(12) Kirste, R. G.; Oberthür, R. C. In "Small Angle X-ray Scattering"; Glatter, O., Kratky, O., Eds.; Academic Press: London, 1982; pp 387-431.
(13) Cotton, J. P.; Nierlich, M.; Boué, F.; Daoud, M.; Farnoux, B.; Jannink, G.; Duplessix, R.; Picot, C. *J. Chem. Phys.* **1976**, *65*, 1101.
(14) Porod, G. In "Small Angle X-ray Scattering"; Glatter, O., Kratky, O., Eds.; Academic Press: London, 1982; pp 17-51.
(15) Kostorz, G. "Small Angle X-ray Scattering"; Glater, O., Kratky, O., Eds.; Academic Press: London, 1982; pp 467-498.
(16) Schaefer, D. W.; Keefer, K. D. *Phys. Rev. Lett.* **1984**, *53*, 1383.
(17) Mandelbrot, B. "The Fractal Geometry of Nature"; W. H. Freeman: San Francisco, 1982.

Polyurethane Interpenetrating Polymer Networks (IPN's) Synthesized under High Pressure. 4. Compositional Variation of Polyurethane–Polystyrene IPN's and Linear Blends

Doo Sung Lee

Department of Textile Engineering, Sung Kyun Kwan University, Suwon, Kyungki 170, Republic of Korea

Sung Chul Kim*

Department of Chemical Engineering, Korea Advanced Institute of Science and Technology, Chongyangni, Seoul 131, Republic of Korea. *Received January 30, 1985*

ABSTRACT: A series of interpenetrating polymer networks and linear blends of polyurethane–polystyrene with different compositions were synthesized under high pressure. The relative order of the degree of mixing of the IPN's was PU75PS25, PU50PS50, and PU25PS75. The dynamic complex modulus behavior followed the theoretical model of Budiansky, which showed phase inversion when the IPN's were synthesized at atmospheric pressure, and followed the Dickie model with glassy matrix when synthesized at 10 000 kg/cm^2 pressure. The morphology via transmission electron microscopy agrees well with the glass transition and modulus behavior. The increased density of IPN's synthesized at high pressure is due to the increase of the degree of mixing and the densification of the polystyrene network. The swelling data indicate that there might be some effect of the interactions caused by the interpenetration of the PU and PS network.

Introduction

Interpenetrating polymer networks (IPN's) can be defined as a mixture of two or more cross-linked polymer networks that have partial or total physical interlocking between them. This subject has been reviewed several times recently.[1-3] The incompatibility of the IPN's arises from the usually low entropy of mixing obtained on blending the high molecular weight polymers, like other polyblend systems. The interpenetration plays a significant role in enhancing the compatibility of the polymer components due to the fact that the physical interlocking prohibits the phase separation from occurring.[4] IPN's exhibit varying degrees of phase separation depending, primarily, on the respective compatibilities of the constituent polymers and, secondly, on the relative rate of network formation and the rate of phase separation.[5] The rate of phase separation is controlled by the mobility of the polymer segment and is related to T_g, molecular weight, and synthesis temperature and pressure.

In the previous papers of this series,[5-7] the synthesis pressure and temperature effects on the miscibility and properties of PU–PMMA IPN's, PU–PS IPN's, semi-IPN's, and linear blends were discussed. The phase separation mechanism when the IPN's were synthesized under high pressure was proposed with relation to the Gibb's free energy of mixing, conversion, the mobility of the polymer segment, and cross-link density. The effect of physical interlocking characteristics was also illustrated. However, the composition of the component polymers was held at 50/50% by weight in the previous papers.

In this paper, the properties of the polyurethane–polystyrene IPN's and linear blends with compositional variations will be discussed.

Experimental Section

Synthesis. The synthesis of the polyurethane–polystyrene IPN's and linear blends was reported elsewhere.[5,7] The PU component was formed by reacting poly(tetramethylene ether) glycol–MDI prepolymer with chain extender (1:1 equivalent ratio of 1,4-butanediol and trimethylolpropane). The cross-linking agent of the PS network was divinylbenzene (55% purity reagent, 2.5 wt % in styrene monomer). The cross-link densities of both networks were set at $\bar{M}_c$ = 3200. The linear blends were formed by excluding the appropriate cross-linking agents in both component polymer formulations. The PU component was reacted at room temperature for 24 h for partial polymerization before the high-pressure reaction. This could be considered to be a kind of SIN with a different polymerization rate. The method of high-pressure synthesis was the same as described before.[5,7] The samples were coded for convenience of presentation. The first

0024-9297/85/2218-2173$01.50/0